Optimization-based identification of potential for demand-side management

Björn Bahl[a], Philip Voll[b] and André Bardow[c]

[a-c] Chair of Technical Thermodynamics, RWTH Aachen University, Aachen, Germany,
[a] bjoern.bahl@ltt.rwth-aachen.de
[b] philip.voll@ltt.rwth-aachen.de
[c] andre.bardow@ltt.rwth-aachen.de ***(CA)***

Abstract:

A methodology is presented for the systematic identification of demand-side management (DSM) potential using mathematical programming techniques. For optimization of energy supply system (ESS), energy demands are usually considered as fixed constraints. However, assuming fixed demands leads to economically suboptimal solutions for the overall system. Thus, DSM measures should be integrated into the design of energy supply systems.

DSM measures are—by definition—demand- and thus case-specific. Therefore, problem-specific models and tools are required to achieve the integrated design of energy demand and supply. In this work, we present a methodology simultaneously considering supply and demand side, without requiring an integrated model. This methodology provides guidance for process engineers by identifing time steps with large potential for cost reduction through DSM.

The proposed method consists of two steps motivated by the two dimensions of a demand profile: 1. At what time is it most valuable to reduce the demand? 2. How much energy demand reduction is most valuable? To identify the most promising time steps for DSM measures, the derivative of the objective function is evaluated. Subsequently, the identified time steps are analysed to determine the optimal amount of the demand reduction by maximizing the improvements of the objective function. The improvement in the objective function quantifies the DSM potential. The presented approach allows to employ a detailed mathematical model of the ESS accounting for time-varying load profiles, continuous equipment sizing, and part-load dependent operating efficiencies. In contrast, the process model is represented in a very simplified way by variations of the demand time series. Thus, the presented approach is applicable to various process domains without the need for detailed process knowledge.

The benefits of the novel methodology are illustrated for an industrial real-world example. In particular, counterintuitive results are obtained such as time steps where demand reductions lead to increased cost. In summary, the presented methodology guides the process engineer towards cost savings through process modifications based on well-founded optimization results.

Keywords:

Demand-Side Management, Energy Supply Systems, Optimization, Process Systems.

1. Introduction

We present an optimization-based methodology for the systematic identification of potential for cost savings by demand-side management (DSM) in energy systems. Energy systems consist of the energy supply system (ESS) and the process system (PS) (Fig. 1): The energy supply system converts primary and secondary energy to final energy flows required by the process system. The process system employs the provided energy in technical processes, e.g., manufacturing or heating. Today, energy supply system and process system are usually assumed to interact via a fixed interface: The process requests fixed demands (heating, cooling, electricity, etc.) from the ESS; the requested energy flows are provided by the energy supply system as fixed constraints. Fixing demands allows for analysing the energy supply system and process system independently. Independent analysis of both systems is less complex and allows the use of domain-specific tools. In practice, energy supply system and process system are usually anyhow operated by separate

divisions in a company (or even two separate companies) with different decision makers. However, an independent analysis of the ESS and the PS neglects any synergies, and thus usually leads to suboptimal solutions for the overall energy system. Hence, for an optimal overall energy system design, ESS and PS should be considered simultaneously [**1**, **2**].

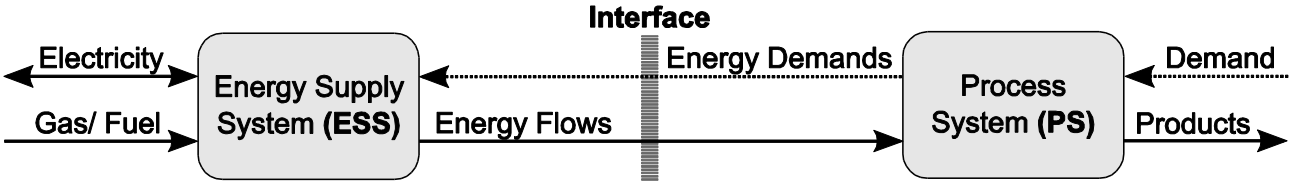

Fig. 1. A general energy system consists of two sub-systems: Energy supply system and process system. A fixed interface is usually assumed between the two sub-systems allowing for independent optimization. The independent analysis neglects interactions between the sub-systems yielding a suboptimal solution for the complete energy system.

To overcome the limitation of an independent analysis, energy storage is commonly introduced in the system model at the interface between the two sub-systems (ESS and PS) to still allow for decoupled analysis and optimization [**3**, **4**]. Considering degrees of freedom of the PS in the design of ESS is commonly referred to as demand-side management (DSM). The potential and opportunities of DSM are well known and widely discussed in literature especially for electricity markets and grids [**5**, **6**, **7**]; in this context, smart- or intelligent grids are intensively addressed [**8**, **9**]. The DSM concept can also be transferred to other utilities such as heating demand [**10**, **3**]. However, integrating the analysis of ESS and PS into one holistic optimization model [**11**, **12**] requires a large and case-specific model of the process and thus limits the level of detail in the model. In particular, a new model of the process system needs to be developed for every design task. In contrast, the energy supply system will be very similar for a wide variety of applications.

In this paper, we present a methodology simultaneously considering the energy supply system and process system to systematically identify DSM potential without requiring an integrated, problem-specific process model. The process system is considered on a generic level ensuring the reusability of the described methodology for very different applications. In contrast, a detailed model [**13**] is employed for the energy supply system, as the energy supply system is similar for different applications. The detailed model accounts for time-varying load profiles, continuous sizing of equipment and part-load dependent operating efficiencies. The aim of the described methodology is to enable synergies between the supply- and the demand-side by identifying potential for cost savings through DSM based on an independently optimized ESS. Our approach determines the most promising time steps for DSM, the optimal size of DSM measures, and quantifies potential savings. Based on this information, the energy systems operator/designer could guide the process engineer to exploit promising process modifications.

In Section 2, the proposed methodology is introduced together with the employed mixed-integer linear program (MILP) model. In Section 3, the methodology is illustrated for a real-world problem. Conclusions are drawn in Section 4.

2. DSM potential in optimization of energy supply systems

The proposed methodology systematically identifies potential for more efficient energy use through DSM measures. The analysis is based on an independently optimized energy supply systems. The methodology consists of two steps addressing the two dimensions of a demand profile (Fig. 2) by answering two questions: First, *at what time* is it (most) valuable to reduce the demand? Second, *how much* energy demand reduction is (most) valuable? Accordingly, in the first step, promising time steps are identified by evaluating the derivative of the objective function with respect to the corresponding demands. In our approach, we assume that the time steps with the largest derivative

are most promising for DSM measures. If an economic objective is used, the derivative corresponds to the marginal costs. Marginal costs have successfully been used by Lozano et al. [14] to describe different operation modes of a trigeneration system. However, local information at the optimal design point of the ESS is not sufficient to quantify the DSM potential. Therefore, in the second step of the proposed methodology, improvements in the objective are evaluated as a function of the amount the energy demand is reduced. For the evaluations, a detailed model of the ESS is used.

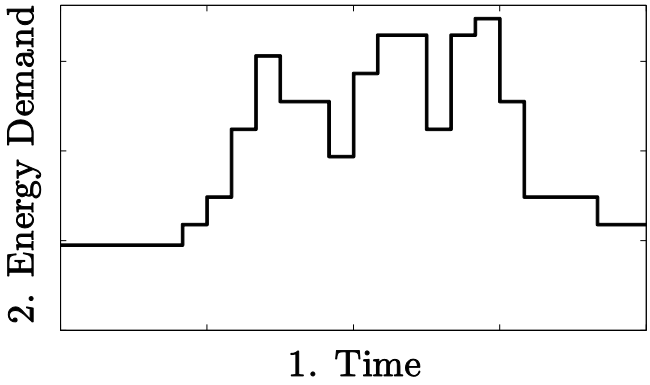

Fig. 2. The two dimensions of a demand profile motivate the two steps of the proposed methodology: 1. At what time *is it (most) valuable to reduce the demand? 2.* How much *energy demand reduction is (most) valuable?*

2.1. MILP model for ESS optimization

Our approach is based on the optimization of energy supply systems. While the suggested approach is generic, we here employ the MILP model presented by Voll et al. [13]. The objective function f is assumed to be minimized without any loss of generality:

$$f^* := \min_{\dot{V}_n^N, \dot{V}_{nt}, y_n, \delta_{nt}} f\left(\dot{V}_n^{\mathrm{N}}, \dot{V}_{nt}, y_n, \delta_{nt}\right) \tag{1}$$

$$\text{s.t.} \sum_{n=1}^{n_{\max}} \dot{V}_{nt} = \dot{E}_t, \forall t \in \{t_1, ..., t_{\max}\}, \forall \text{demands}, \tag{2}$$

$$\dot{V}_n^{\mathrm{N}} \in \mathbb{R}^{n_{\max}}, \dot{V}_{nt} \in \mathbb{R}^{n_{\max} \times t_{\max}}, y_n \in \{0,1\}^{n_{\max}}, \delta_{nt} \in \{0,1\}^{n_{\max} \times t_{\max}}.$$

The continuous degrees of freedom $\dot{V}_{nt}$ and $\dot{V}_n^{\mathrm{N}}$ represent the operation in time step t of component n as well as the nominal capacity of component n, respectively. The binary degrees of freedom y_n and δ_{nt} represent whether the component n is build and operated in time step t, respectively. The components have to meet the energy demands $\dot{E}_t$ (heating, cooling and electricity) for every time step t, Eq. (2). Moreover, minimum and maximum nominal capacity limits, linearized part-load performance curves, minimum part load operation, and linearized investment cost functions are considered in the model (for equations: see Appendix A). The equipment considered in this work encompasses gas-fueled boilers and gas engines, electricity-driven turbo-compression chillers, and thermally driven absorption chillers.

2.2. Step 1: Time steps with high DSM potential

Our approach is initialized by the design point $f^*\left(\dot{E}_t\right)$ of the optimized energy supply system. The derivative of the objective function is calculated with respect to reduction of the energy demand. The derivative is evaluated for each time step t of all demand profiles; it determines the sensitivity of the objective function to the amount the energy demand is reduced, the so-called reduction level $\Delta\dot{E}_t$. Here, the derivative is approximated by finite differences

$$\frac{\mathrm{d}f^*\left(\Delta\dot{E}_t\right)}{\mathrm{d}\left(\Delta\dot{E}_t\right)} \approx \frac{f^*\left(\dot{E}_t - \Delta\dot{E}_t\right) - f^*\left(\dot{E}_t\right)}{\Delta\dot{E}_t}, \forall t, \forall \text{demands} . \quad (3)$$

For minimization problems, a negative derivative with respect to demand reductions indicates improvements in the objective function. Improvements in the objective function by demand reductions represent potential for DSM measures. Thus, time steps with high negative derivatives have high DSM potential and are selected as most promising time steps t_p.

The selection of t_p is based on the derivative $\frac{\mathrm{d}f^*\left(\Delta\dot{E}_t\right)}{\mathrm{d}\left(\Delta\dot{E}_t\right)}$ of the objective function for the reference demands $\dot{E}_t$, i.e. in the limit $\Delta\dot{E}_t = 0$. For higher reduction levels $\Delta\dot{E}_t$, this derivative can change. Selecting the highest derivatives at $\Delta\dot{E}_t = 0$ is thus a heuristic assuming a concave dependency of the DSM potential on the reduction levels $\Delta\dot{E}_t$.

In summary, step 1 of the proposed methodology answers the question: *At what time* is it (most) valuable to reduce the demand? The selection can be done for a fixed number of time steps with the highest negative derivatives, or a threshold can be defined for the derivative, below which all time steps are selected.

2.3. Step 2: Improvement of objective function

In step 2 of the proposed methodology, the time steps t_p identified in step 1 are analysed in more detail. The goal is to determine how much the energy demand should be reduced. To quantify the DSM potential, improvements of the objective function value Δf^* are obtained depending on the demand reduction level $\Delta\dot{E}_t$. The improvements Δf^* are determined by the difference between the optimal objective function values for the reduced energy demand $f^*\left(\dot{E}_t - \Delta\dot{E}_t\right)$ and for the reference energy demand $f^*\left(\dot{E}_t\right)$

$$\Delta f^*\left(\Delta\dot{E}_t\right) = f^*\left(\dot{E}_t - \Delta\dot{E}_t\right) - f^*\left(\dot{E}_t\right), \forall t_\mathrm{p} \quad (4)$$

The improvements of the objective function Δf^* provide information about *how much* energy demand reduction $\Delta\dot{E}_t$ is (most) valuable for the identified time steps.

2.4. Decisions in operation- and structure optimization

The decisions taken in energy systems optimization depend on the objective of the study. In general, we distinguish between optimization of operation and structure [15]. These two classes of optimization differ in time horizons and decision options (Table 1). For the identification of DSM potential, the two optimization classes differ in the possible improvements and thus in DSM potential. For illustration, consider a change in the peak demand: The possible investment in a new component to meet this peak demand is conceptually different from changes in the operation of an existing energy supply system. Still, the described methodology handles both optimization of operation and structure.

Table 1. Difference between optimization of operation and structure: Time horizon and possible decision including degrees of freedom.

	Operation Optimization	Structure Optimization
Time horizon	Days – year	Years – decades
Decisions	Operation of components: $\dot{V}_{nt}, \delta_{nt}$	Structure of ESS and operation of components: $\dot{V}_n^\mathrm{N}, y_n, \dot{V}_{nt}, \delta_{nt}$

3. Illustrative case study

The presented methodology is illustrated based on an industrial real-world case study (for details see Appendix A and [13]). The cooling, heating and electricity demand are considered for different buildings (e.g., production, laboratory, facilities, offices, etc.). Two 24 hour-based scenarios are analysed (Fig. 3): Scenario "North" (N) has high heating demand compared to the cooling demand, whereas the cooling demand in Scenario "South" (S) is higher than the heating demand.

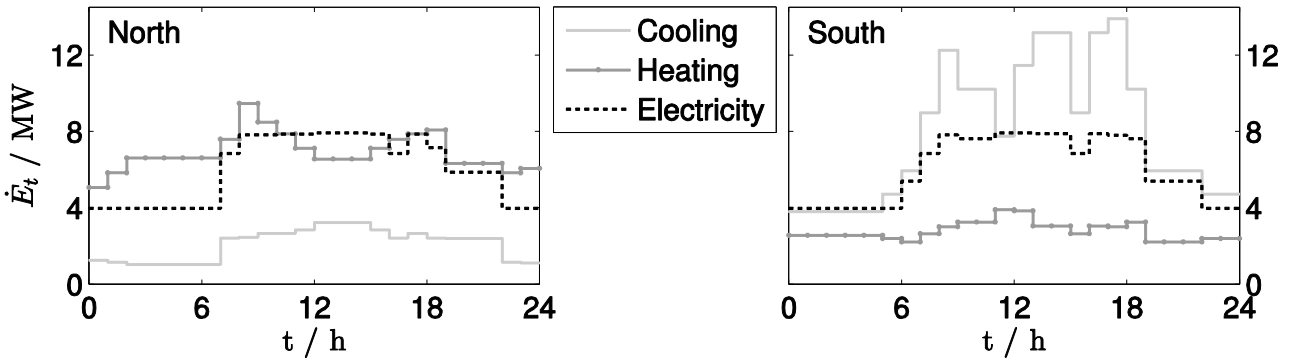

Fig. 3. Energy demand profiles $\dot{E}_t$ (Cooling, heating and electricity) for time steps t of an industrial real-world case study: Two 24 hour-based scenarios are selected: Scenario "North" (left) with high heating demand compared to the cooling demand and Scenario "south" (right) with high cooling demand compared to the heating demand.

The total annualized costs (TC) of the energy supply system are considered as objective function (Eq. (1)). TC reflects the trade-off between energy costs and annualized investment cost in a single objective optimization

$$\min_{\dot{V}_n^{\mathrm{N}},\dot{V}_{nt},y_n,\delta_{nt}} TC = \sum_{n=1}^{n_{\max}}\sum_{t=1}^{t_{\max}} p_{\mathrm{Un}}\Delta t_t \cdot \dot{U}_{nt}\left(\delta_{nt},\dot{V}_n^{\mathrm{N}},\dot{V}_{nt}\right) - \frac{i(i+1)^{t_{TC}}}{(i+1)^{t_{TC}}-1}\cdot\sum_{n=1}^{n_{\max}} I_n\left(y_n,\dot{V}_n^{\mathrm{N}}\right), \qquad (5)$$

where $\dot{U}_{nt}$ is the input energy flow to unit n in time step t and I_n the investment cost for unit n. p_{Un} is the specific cost of the input energy flow of component n (i.e., p_U^{gas} or $p_U^{electricity}$) and Δt_t the time interval of time step t. The annualized investment costs are based on the interest rate i for the time horizon t_{TC}. TC enables a comparison of the optimization of operation and structure (Sec. 2.4.). To initialize our approach, we determine the optimal solution for the reference demand profiles: For the Scenario North the optimal structure is a complex trigeneration system consisting of one absorption chiller (AC), three compression chillers (CC), two boilers (B) and three combined heat and power (CHP) units (Table 2). The total annualized costs objective is 8.5 Mio€. The optimal structure for Scenario South consists of two AC, five CC and three CHP units (Table 2). The total annualized costs objective is 8.9 Mio€.

Table 2. Nominal size $\dot{V}_n^{\mathrm{N}}$ / MW and technology of the optimal structure of the ESS for Scenario North and Scenario South. (AC – adsorption chiller, CC – compression chiller, B – boiler, CHP – combined heat and power)

Technology	AC	AC	CC	CC	CC	CC	CC	B	B	CHP	CHP	CHP
North: $\dot{V}_n^{\mathrm{N}}$ / MW	0.35	-	0.90	1.75	0.70	-	-	1.60	0.76	2.51	2.30	2.30
South: $\dot{V}_n^{\mathrm{N}}$ / MW	3.87	1.89	1.10	0.50	4.05	2.74	1.58	-	-	3.05	2.50	2.50

3.1. Step 1: Identification of promising time steps for DSM

Step 1 of the presented methodology (Sec. 2.2.) identifies promising time steps with high DSM potential. The derivative of the objective function with respect to the demand in the corresponding time step t is here marginal annual costs $\frac{\mathrm{d}TC^*}{\mathrm{d}\left(\Delta\dot{E}_t\right)}$.

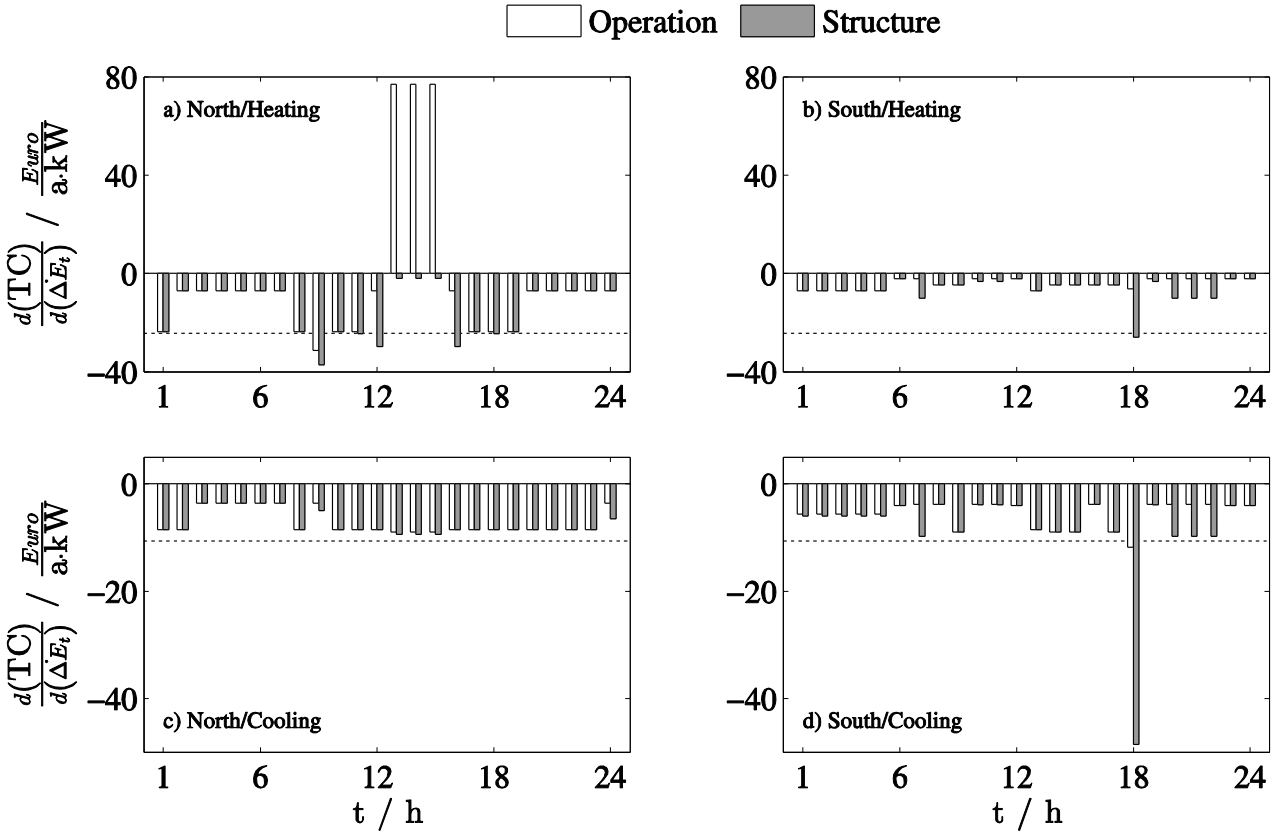

Fig. 4. The derivative of objective function TC with respect to the heating demand (top row) and cooling demand (bottom row) is shown to identify promising time steps t_p with high DSM potential, i.e. high negative derivatives. All time steps of Scenario N (left column) and Scenario S (right column) are evaluated considering optimization of operation (white bars) and structure (grey bars). A benchmark (dashed line) based on the common way to provide the energy flow with separate production is provided to give an orientation on the value of the derivative.

In most time steps, we observe negative derivatives indicating DSM potential; even though the potential for DSM measures is small for some time steps. Therefore, a benchmark (dashed line) is provided to give an orientation on the value of the derivative, i.e., the DSM potential. The benchmark is based on the common way to provide the corresponding energy flow in separate generation: For the heating demand (top row), a boiler at nominal efficiency is the benchmark and the benchmark for the cooling demand (bottom row) is a compression chiller at nominal coefficient of performance.

We observe a wide range of the derivative: from values slightly below zero to very high negative values. Thus, we classify the observed cases by comparing them to the benchmark; the cases are ordered by decreasing DSM potential starting with the highest:

The derivative is more negative than the benchmark (Derivative < Benchmark):

This condition is fulfilled at peak demand points for each scenario (Fig 4a: 9 h; Fig 4d: 18 h) for both optimization of operation and structure. The peak demands are an intuitive choice for time steps with high DSM potential and are also detected by the presented methodology, but without any need of heuristic knowledge. However, high DSM potential is also identified by the proposed

methodology at unexpected time steps (Fig 4a: 12h and Fig 4b: 18h, structure optimization). In optimization of operation, DSM potential is high due to better utilization of the trigeneration in the ESS: The demand-ratio approaches the characteristic of the trigeneration system. For structure optimization, additionally, smaller equipment can be selected.

Derivative ≈ Benchmark:

In the corresponding time steps, parts of the demand are provided by the benchmark technology, operated near its nominal efficiency. The co-/trigeneration system is not affected by a reduction of the energy demand, such that there is no negative effect on the supply of other demands. Hence, the DSM potential is high.

Benchmark < Derivative < 0:

These conditions have less cost savings potential for DSM. We observe that this case occurs if cogeneration is operating in the reference solution. If one demand type is reduced, this result in cost savings, but the demand-ratio diverges from the characteristic of the co-/trigeneration resulting in extra costs for the extra supply of other energy types. Thus, the overall DSM potential is smaller due to negative effects on the co-/trigeneration in the ESS.

0 < Derivative:

A positive derivative indicates additional cost for a reduction of the energy demand (Fig 4a: 14h); this behaviour is counter-intuitive. It is observed at time steps with low heating- and high cooling demand. For these time steps the operation and design of the ESS is critical: Heat is completely supplied by the CHP units; hence reducing the heating demand results in less produced electricity to meet the electricity demand. As the ACs are operated at maximum load, the trigeneration cannot compensate this heating demand reduction either; thus, in this time step, heating demand reduction results in less electricity production by the CHP units which forces the system to buy extra electricity from the grid; the cost of electricity is higher than the cost of gas. Hence, this results in negative DSM potential for the heating demand in this time steps.

The value of the derivatives of operation- (white bars) and structure optimization (grey bars, Fig. 4) is equal for many time steps: The structure of the ESS is optimal for both, the original and the reduced demand. Thus, the cost savings and DSM potential are only based on the operation of the ESS. The DSM potential of the optimization of operation represents a minimum for the optimization of structure which considers additional degrees of freedom. Hence, a difference in the DSM potential for optimization of operation and structure can be exploited for the identification of DSM measures resulting in structural changes of the optimal energy supply system and the corresponding time steps are crucial for the design of the ESS.

Positive derivatives are not observed for structure optimization, but the DSM potential for structure optimization is still not significant for time steps with positive derivatives in the operation optimization. Nevertheless, the results from the operation optimization cannot be used to predict DSM potential on the structural level as the results differ significantly in some cases (e.g. Fig 4a: 12 h; Fig 4d: 7 h).

According to the methodology (Sec. 2.2.), the time steps t_{p} with the highest DSM potential are selected based on the highest negative derivatives and further analysed in step 2 of the proposed methodology.

3.2. Step 2: Cost savings and reduction level

In step 2 of the presented methodology, the most promising time steps t_{p} with the highest DSM potential identified by step 1 are investigated: For Scenario North, the largest derivatives are observed at 9 h and 14 h for heating- and cooling demand reduction respectively; in Scenario South the most promising time step is the same (18 h) for heating and cooling thus the second highest (7 h) is also selected. As introduced in Sec. 2.3., the possible cost savings ΔTC are calculated for the

selected time steps as a function of the demand reduction level $\Delta\dot{E}_t$ (Fig. 5). The results are only shown for a selection of the identified time steps to exemplify the observed trends.

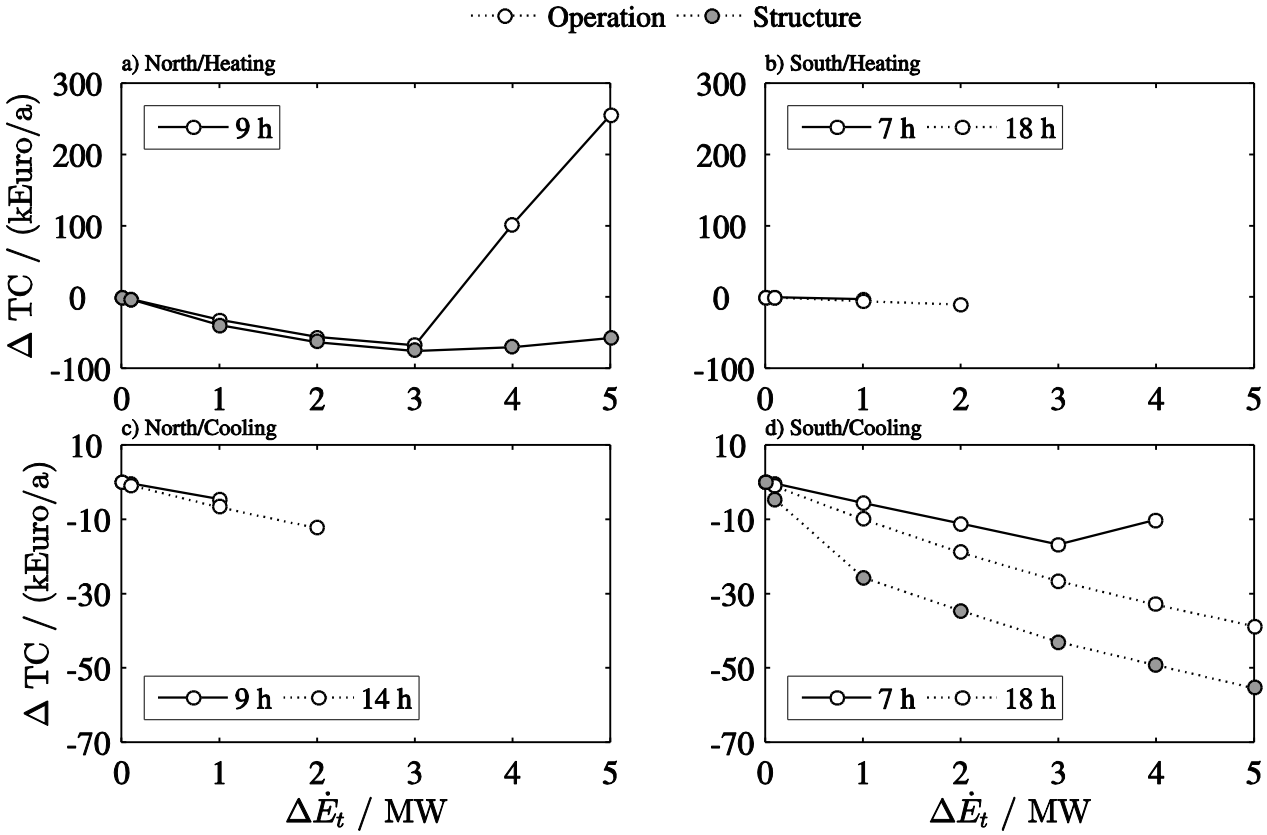

Fig. 5. Cost savings as a function of the reduction level $\Delta\dot{E}_t$ for promising time steps t_p. Time steps from Scenario N (left column) and Scenario S (right column) are investigated for heating- (top row) and cooling demand (bottom row) reduction. The results are presented for a selection of the identified time steps to show the observed trends. Operation optimization (white bars) instances and structure optimization (grey bars) are shown.

We observe different trends of the DSM potential depending on the reduction level: As a first type of trend, we see monotone decreasing objective functions, i.e., every demand reduction results in additional cost savings. This trend is found for heating demand reductions in Scenario South (Fig. 5b) and cooling demand reductions in Scenario North (Fig. 5c) as well as for some cooling demand reductions in Scenario South (Fig. 5d: 18h, operation). Second, cases are observed with minima in the DSM potential: Further reduction of the demand can diminish cost savings (e.g. Fig 5d: 7 h, operation) and eventually lead to additional cost (e.g. Fig 5a: 9 h, operation) if the demand is reduced even more. The high heating demand reduction results in higher usage of the CCHP capacity in the system. If the adsorption chiller is operated at maximum a reduction of the heating demand results in less produced heat of the CHP engine and thus less produced electricity, which in turn needs to be bought from the grid. In sum, this results in extra cost for the energy supply. Thus, for these cases an optimal reduction level exists and a DSM measure should be limited to this reduction level.

Moreover, all functions of the DSM potential are concave as assumed in step 1 (also for the time steps not shown). Thus, the identification of high DSM potential by a large derivative of the objective function at the reference demand $\frac{\mathrm{d}TC^*}{\mathrm{d}\left(\Delta\dot{E}_t\right)}$ is reasonable (Sec. 2.2.).

A decreasing DSM potential and optimal reduction levels are observed for both operation- and structure optimization. The magnitude of cost savings for structure optimization results in higher

potential for all time steps and reduction levels due to the possibility of investment cost savings. The DSM potential for investment costs saving can be measured by the difference between the operation and structure optimization values (white and grey).

4. Conclusions

An optimization-based methodology is presented for the systematic identification of DSM potential in energy systems. Today, the two subsystems of an energy system (energy supply system and process system) are usually assumed to interact via a fixed interface and therefore analysed and optimized separately. The presented methodology considers the two sub-systems of an energy system simultaneously, but does not require an integrated model of the process system. In contrast, a detailed model of the energy supply system is employed as the ESS is very similar for different applications. Hence, the approach is applicable to various energy systems without detailed knowledge of the process.

The presented methodology is applied to a real-world case study. The results show that methods for the systematic identification of DSM potential are needed to answer the question, *at what time* energy demand reduction is most valuable: Beside the time steps with demand peaks, non-intuitive time steps with high cost savings potential through DSM measures are identified by the proposed optimization-based methodology. Moreover, time steps are identified by the methodology for which a demand reduction results in additional cost. Hence, a heuristic just focusing on the demand peaks is not sufficient to identify time steps with high DSM potential.

Subsequently, the methodology determines h*ow much* energy demand reduction is most valuable: Besides monotone increasing cost saving potential for higher energy demand reductions, some cases show an optimal reduction level: Higher energy demand reduction can diminish cost savings and can lead to additional cost in extreme cases. Therefore, the best amount of energy demand reduction by DSM measures needs to be determined by a systematic methodology.

The proposed methodology is generic and thus capable to be applied to various energy systems optimization models to identify and quantify the system-inherent potential for DSM measures.

Acknowledgments

Parts of this study were funded by the German Federal Ministry for Economic Affairs and Energy (ref. no.: 03ET1259A). The support is gratefully acknowledged.

Appendix A

This section describes the employed MILP model by Voll et al. [13], which is used for the illustrative case study in Chapter 3. In this model, several energy conversion technologies (Table A.1.) are considered for the design of the energy supply system.

Table A.1. The considered technologies with their thermal power range, investment cost range, maintenance cost and nominal coefficient of performance or nominal efficiency.

technology	thermal power range / MW	investment cost / k€	Maintenance cost / % investment cost	η_n^N, COP_n^N / -
Boiler	0.1 - 14.0	34 - 380	1.5	0.90
CHP engine	0.5 - 3.2	230 - 850	10.0	0.87
Adsorption chiller	0.1 - 6.5	75 - 520	4.0	0.67
Turbo chiller	0.4 - 10.0	89 -1570	1.0	5.54

The investment cost curves are linearized by piecewise linear functions, for all components n and every segment h the y-intercept I_{nh} and the gradient $\left(\frac{dI}{d\dot{V}^N}\right)_{nh}$ are given as parameters. $\tilde{\dot{V}}_{nh}^N$ is a

continuous degree of freedom representing the nominal output power of a segment and γ_{nh} is a binary degree of freedom identifying weather the nominal output power is in the corresponding segment of the piecewise linear function:

$$I_n\left(y_n, \dot{V}_n^{\mathrm{N}}\right) = \sum_{h=1}^{h_{\max}} \left(\gamma_{nh} \cdot I_{nh} + \tilde{\dot{V}}_{nh}^{\mathrm{N}} \cdot \left(\frac{dI}{d\dot{V}^{\mathrm{N}}} \right)_{nh} \right), \forall n, \tag{A.1}$$

$$y_n = \sum_{h=1}^{h_{\max}} \left(\gamma_{nh}\right) \leq 1, \forall n, \tag{A.2}$$

$$\gamma_{nh} \cdot \tilde{\dot{V}}_{nh}^{\mathrm{N,min}} \leq \tilde{\dot{V}}_{nh}^{\mathrm{N}} \leq \gamma_{nh} \cdot \tilde{\dot{V}}_{nh}^{\mathrm{N,max}}, \forall h, \forall n, \tag{A.3}$$

$$\tilde{\dot{V}}_{nh}^{\mathrm{N}} \in \mathbb{R}^{n_{\max} \mathrm{x}\, h_{\max}}, \gamma_{nh} \in \{0,1\}^{n_{\max} \mathrm{x}\, h_{\max}},$$

where $\tilde{\dot{V}}_{nh}^{\mathrm{N,min}}$ and $\tilde{\dot{V}}_{nh}^{\mathrm{N,max}}$ are parameters representing the limits of the corresponding segment. Moreover, the part-load performance curves are represented by piecewise linear functions. Again, for all components n and every segment g, the normalized y-intercept u_{ng} and the normalized gradient $\left(\frac{du}{dv}\right)_{ng}$ are given as parameters. $\tilde{\dot{V}}_{ntg}$ is continuous degree of freedom representing the output power of a segment and $\tilde{\delta}_{ntg}$ is a binary degree of freedom identifying whether the output power is in the corresponding segment of the piecewise linear function:

$$\dot{U}_{nt}\left(\delta_{nt}, \dot{V}_n^{\mathrm{N}}, \dot{V}_{nt}\right) = \sum_{g=1}^{g_{\max}} \left(\tilde{\delta}_{ntg} \cdot u_{ng} \cdot \frac{\dot{V}_n^{\mathrm{N}}}{\eta_n^{\mathrm{N}}} + \tilde{\dot{V}}_{ntg} \cdot \left(\frac{du}{dv} \right)_{ng} \cdot \frac{1}{\eta_n^{\mathrm{N}}} \right), \forall t, \forall n, \tag{A.4}$$

$$\delta_{nt} = \sum_{g=1}^{g_{\max}} \tilde{\delta}_{ntg} \leq 1, \forall t, \forall n, \tag{A.5}$$

$$\tilde{\delta}_{ntg} \cdot \dot{V}_n^{\mathrm{N}} \cdot v_{\min} \leq \tilde{\dot{V}}_{ntg} \leq \tilde{\delta}_{ntg} \cdot \dot{V}_n^{\mathrm{N}}, \forall g, \forall t, \forall n. \tag{A.6}$$

$$\tilde{\dot{V}}_{ntg} \in \mathbb{R}^{n_{\max} \mathrm{x}\, t_{\max} \mathrm{x}\, g_{\max}}, \tilde{\delta}_{ntg} \in \{0,1\}^{n_{\max} \mathrm{x}\, t_{\max} \mathrm{x}\, g_{\max}}.$$

The bilinear product $\tilde{\delta}_{ntg} \cdot \dot{V}_n^{\mathrm{N}}$ in Eq. A.4 and Eq. A.6 can be linearized according to Petersen [16] and [17]. For simplification, this is illustrated for $g = 1$, thus $\tilde{\delta}_{ntg} = \delta_{nt}$. The bilinear product is substituted by an auxiliary continuous decision variable ξ_{nt}, therefore we need to introduce a time dependent variable ψ_{nt} that takes the values of $\dot{V}_n^{\mathrm{N}}$ for all time steps t

$$\psi_{nt} = \dot{V}_n^{\mathrm{N}}, \forall t, \forall n, \tag{A.7}$$

Now $\dot{V}_n^{\mathrm{N}}$ is substituted by ψ_{nt} in Eq. (A.1) - (A.6) and the bilinear product $\delta_{nt} \cdot \psi_{nt}$ is substituted by ξ_{nt}. Two linear constraints are added to guarantee the correct behaviour of ξ_{nt}:

$$\delta_{nt} \cdot \dot{V}_{\min}^{\mathrm{N}} \leq \xi_{nt} \leq \delta_{nt} \cdot \dot{V}_{\max}^{\mathrm{N}}, \forall t, \forall n, \tag{A.8}$$

$$\left(1 - \delta_{nt}\right) \cdot \dot{V}_{\min}^{\mathrm{N}} \leq \psi_{nt} - \xi_{nt} \leq \left(1 - \delta_{nt}\right) \cdot \dot{V}_{\max}^{\mathrm{N}}, \forall t, \forall n. \tag{A.9}$$

The thermal and electrical nominal efficiency of the CHP engine is a function of the engine size, to capture this behaviour, the CHP model is portioned into size depended sub models:

- Small: 0.5…1.4 MW, $\eta^{\mathrm{N,th}} = 0.460, \eta^{\mathrm{N,el}} = 0.410$
- Medium: 1.4…2.3 MW, $\eta^{\mathrm{N,th}} = 0.424, \eta^{\mathrm{N,el}} = 0.446$

- Large: 2.3…3.2 MW, $\eta^{\mathrm{N,th}} = 0.388, \eta^{\mathrm{N,el}} = 0.482$

To ensure that only one equipment size is selected, a constraint is added:

$$y_{\mathrm{Small}} + y_{\mathrm{Medium}} + y_{\mathrm{Large}} \leq y, \forall n \in \mathrm{CHP}\,. \qquad \text{(A.10)}$$

References

[1] Grossmann IE., Challenges in the application of mathematical programming in the enterprise-wide optimization of process industries. Theor Found Chem Eng. 2014;48(5):555–573.

[2] Kravanja Z., Challenges in sustainable integrated process synthesis and the capabilities of an MINLP process synthesizer MipSyn. Comput Chem Eng. 2010;34(11):1831–1848.

[3] Christidis A., Koch C., Pottel L., Tsatsaronis G., The contribution of heat storage to the profitable operation of combined heat and power plants in liberalized electricity markets. Energy. 2012;41(1):75 – 82. 23rd International Conference on Efficiency, Cost, Optimization, Simulation and Environmental Impact of Energy Systems, {ECOS} 2010.

[4] Fazlollahi S., Becker G., Maréchal F., Multi-objectives, multi-period optimization of district energy systems: II-Daily thermal storage. Comput Chem Eng. 2014;71(0):648 – 662.

[5] Gellings CW., The concept of demand-side management for electric utilities. Proceedings of the IEEE. 1985 Oct;73(10):1468–1470.

[6] Strbac G., Demand side management: Benefits and challenges. Energy Policy. 2008;36(12):4419 – 4426. Foresight Sustainable Energy Management and the Built Environment Project.

[7] Warren P., A review of demand-side management policy in the {UK}. Renew Sust Energ Rev. 2014;29(0):941 – 951.

[8] Palensky P., Dietrich D., Demand Side Management: Demand Response, Intelligent Energy Systems, and Smart Loads [Article]. IEEE T Ind Inform. 2011 AUG;7(3):381–388.

[9] Logenthiran T., Srinivasan D., Shun TZ., Demand Side Management in Smart Grid Using Heuristic Optimization [Article]. IEEE T Smart Grid. 2012 SEP;3(3):1244–1252.

[10] Arteconi A., Hewitt NJ., Polonara F., State of the art of thermal storage for demand-side management. Applied Energy. 2012;93(0):371 – 389. (1) Green Energy; (2)Special Section from papers presented at the 2nd International Enery 2030 Conf.

[11] Mitra S., Grossmann IE., Pinto JM., Arora N., Integration of strategic and operational decision-making for continuous power-intensive processes. In: Bogle IDL, Fairweather M, editors. Proceedings of the 22nd European Symposium on Computer Aided Process Engineering. Elsevier; 2011.

[12] Agha MH., Thery R., Hetreux G., Hait A., Lann JML., Integrated production and utility system approach for optimizing industrial unit operations. Energy. 2010;35(2):611–627.

[13] Voll P., Klaffke C., Hennen M., Bardow A., Automated superstructure-based synthesis and optimization of distributed energy supply systems. Energy. 2013;50:374–388.

[14] Lozano MA., Carvalho M., Serra LM., Operational strategy and marginal costs in simple trigeneration systems. Energy. 2009;34(11):2001 – 2008.

[15] Frangopoulos CA., Spakovsky MRv., Sciubba E., A Brief Review of Methods for the Design and Synthesis Optimization of Energy Systems. International Journal of Applied Thermodynamics. 2002 December;5(4):151–160.

[16] Petersen CC., A note on transforming the product of variables to linear form in linear programs; 1971. Working Paper, Purdue University.

[17] Glover F., Improved linear integer programming formulations of nonlinear integer problems. Manag Sci. 1975;22(4):455–460.